

Global polarization of Ξ hyperons in Au+Au collisions in the STAR experiment

Egor Alpatov^a (for the STAR collaboration)¹

^a National Research Nuclear University MEPhI, Kashirskoe highway 31, Moscow,
115409, Russia

Vortical structure of hot-dense matter in heavy ion collisions can be probed through global polarization of emitted particles. Hyperon's weak decays provides opportunity to measure this phenomenon. Global polarization of Λ hyperons was measured by the STAR experiment at RHIC for Au+Au collisions with $\sqrt{s_{NN}} = 3-200$ GeV and at the LHC for Pb+Pb collisions with $\sqrt{s_{NN}} = 2.76$ and 5.02 TeV.

Global polarization of multistrange hyperons, such as Ξ , can provide new information for hydrodynamic description of the system and its vorticity structure. In these proceedings, we report results of Ξ global polarization measurement for Au+Au collisions at $\sqrt{s_{NN}} = 19.6$ and 27 GeV.

Introduction

Ultrarelativistic heavy-ion collisions provide an opportunity to create and examine quark-gluon plasma - hot-dense matter characterized by deconfined state of quarks and gluons. The results from experiments at RHIC and LHC have shown that the expansion dynamics of the quark-gluon plasma (QGP) can be described by relativistic hydrodynamics [1].

Non-central collisions are characterized by vorticity creation in the medium. An experimental indicator of vorticity is the polarization of particles produced in the collision along the direction of the vorticity. This quantity, known as global polarization, can be obtained by studying weak decays of hyperons, in which the daughter particle is emitted predominantly in the direction of its parent spin. [2, 3].

In the hyperon decays the angular distribution of daughter baryons in the parent hyperon rest frame is given by:

$$\frac{dN}{d\cos\theta^*} \propto 1 + \alpha_H P_H \cos\theta^*, \quad (1)$$

α_H is the hyperon decay parameter, P_H is the hyperon polarization, $\cos\theta^*$ is the angle between the polarization vector and daughter baryon momentum in the hyperon rest frame [4].

Initial angular momentum direction is expected to be perpendicular to reaction plane (which is defined by the beam direction and impact parameter vector), and global polarization value can be obtained by measuring daughter baryon's momentum projection on initial angular momentum direction.

¹E-mail: egroker1@gmail.com

28 Assuming first-order event plane as reaction plane, and taking event plane
29 resolution into account:

$$P_H = \frac{8}{\pi\alpha_H} \frac{\langle \sin(\Psi_1^{obs} - \phi_{daughter}^*) \rangle}{Res(\Psi_1)}, \quad (2)$$

30 where $\phi_{daughter}^*$ is the azimuthal angle of the daughter baryon in the parent
31 hyperon rest frame, $Res(\Psi_1)$ is event plane resolution. Decay parameter
32 values are $\alpha_\Lambda = 0.732 \pm 0.014$, $\alpha_{\bar{\Lambda}} = -0.758 \pm 0.010$, $\alpha_{\Xi^-} = -\alpha_{\Xi^+} = -0.401 \pm$
33 0.010 [5].

34 In the STAR experiment global polarization of Λ hyperons was measured
35 for $\sqrt{s_{NN}} = 3 - 200$ GeV [6–8]. While transport and hydrodynamic models
36 successfully describe experimental results, multi-strange hyperons will pro-
37 vide more constraints for the understanding of nature of vorticity. Ξ and Ω
38 global polarization were measured at $\sqrt{s_{NN}} = 200$ GeV [9].

39 Ξ hyperons can be reconstructed by its decay topology $\Xi^- \rightarrow \pi^- + \Lambda \rightarrow$
40 $p + \pi^-$. This cascade decay provides opportunity to measure its global po-
41 larization in two separate ways. One can use Equation 2 to directly measure
42 angle of daughter Λ decaying from Ξ . Additionally, a fraction of Ξ global po-
43 larization could transfer into its daughter Λ polarization with transfer factor
44 $C_{\Xi-\Lambda} = 0.932$ and global polarization of Ξ hyperons could be measured by
45 examining its daughter Λ global polarization [10–12].

46 In this proceedings we report on the measurements of the global polariza-
47 tion of $\Xi^- + \bar{\Xi}^+$ hyperons in Au+Au collisions at $\sqrt{s_{NN}} = 19.6$ and 27 GeV
48 and compare it to that of $\Lambda + \bar{\Lambda}$.

49 Data analysis

50 Data from Au+Au collisions at $\sqrt{s_{NN}} = 19.6$ and 27 GeV collected by
51 STAR experiment as part of Beam-Energy Scan II (BES-II) program were
52 used for this analysis. STAR features cylindrical geometry detector [13].
53 Events that passed minimum-bias trigger with collision vertex within 70 cm
54 from the center of Time-Projection Chamber (TPC) and with vertex position
55 within 2 cm from the beam line in the transverse plane were analyzed.

56 BES-II have detector upgrades compared to that from BES-I [7]. For
57 both $\sqrt{s_{NN}} = 19.6$ and 27 GeV datasets new detector EPD (Event-Plane
58 Detector) [14] was installed, which provides better event-plane resolution
59 due to higher granularity and acceptance than BBC [15]. At $\sqrt{s_{NN}} = 19.6$
60 GeV TPC update (iTPC) was installed with acceptance enhanced by one
61 unit in rapidity. The collision centrality (extent of overlap between colliding
62 nuclei) was determined based on the measured multiplicity of charged tracks
63 within midrapidity region. Centrality and trigger efficiency were obtained by
64 fitting it to a Monte Carlo Glauber simulation.

65 Tracks of charged particles were measured in TPC [16] within a pseudo-
66 rapidity range $|\eta| < 1$ for 27 GeV and $|\eta| < 1.5$ for 19.6 GeV and with full
67 azimuthal acceptance. Pion and proton tracks with momentum > 0.15 GeV/ c

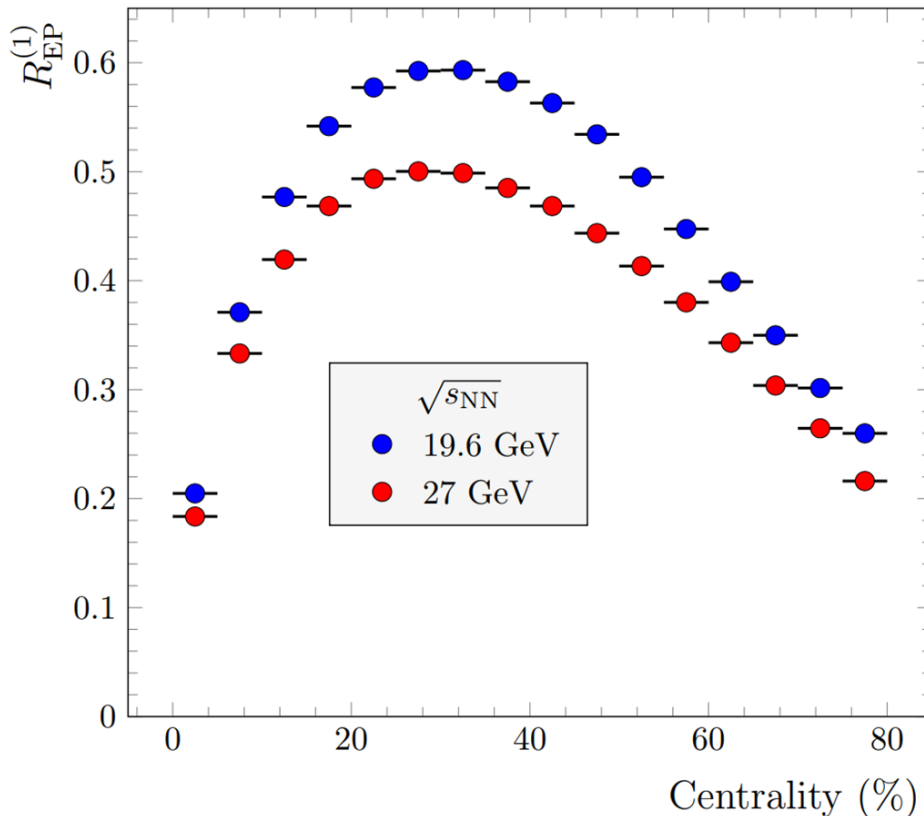


Fig. 1. Resolution of the first order event-plane at $\sqrt{s_{NN}} = 19.6$ and 27 GeV.

68 were identified via energy loss in the TPC, dE/dx , and by their squared mass
 69 obtained by TOF [17] and used for hyperon reconstruction.

70 Λ hyperons were reconstructed via topology of its decay $\Lambda \rightarrow p + \pi^-$
 71 ($\bar{\Lambda} \rightarrow \bar{p} + \pi^+$). After that the same procedure was performed for decay
 72 $\Xi^- \rightarrow \Lambda + \pi$ ($\Xi^+ \rightarrow \bar{\Lambda} + \pi^+$). KFParticle [18] package was used for hyperon
 73 reconstruction.

74 For event plane reconstruction EPD ($2.1 < \eta < 5.1$) and BBC ($3.3 < \eta <$
 75 5.1) were used separately. The first-order event plane of the spectator parti-
 76 cles was used as a proxy for reaction plane. Presented results were obtained in
 77 respect to event-plane measured via EPD, and BBC-measured event-plane
 78 was used for systematic uncertainties estimation. Global polarization cal-
 79 culations with respect to event plane should take into account event plane
 80 resolution. Resolution was calculated via two-subevent method, with the usa-
 81 ge of East (forward rapidity) and West (backward rapidity) detectors, and
 82 is shown in Fig. 1.

83 Following the Equation 2, by taking detector event-plane resolution into
 84 account, global polarization value can be calculated. Track efficiency correc-
 85 tion has negligible impact on polarization and hence not applied. Acceptance
 86 correction, proposed in previous measurements of Λ global polarization, was
 87 applied [7]. Finite detector acceptance leads to small dependence of Equa-
 88 tion 2 from daughter momentum in parent rest frame. For this reason it can

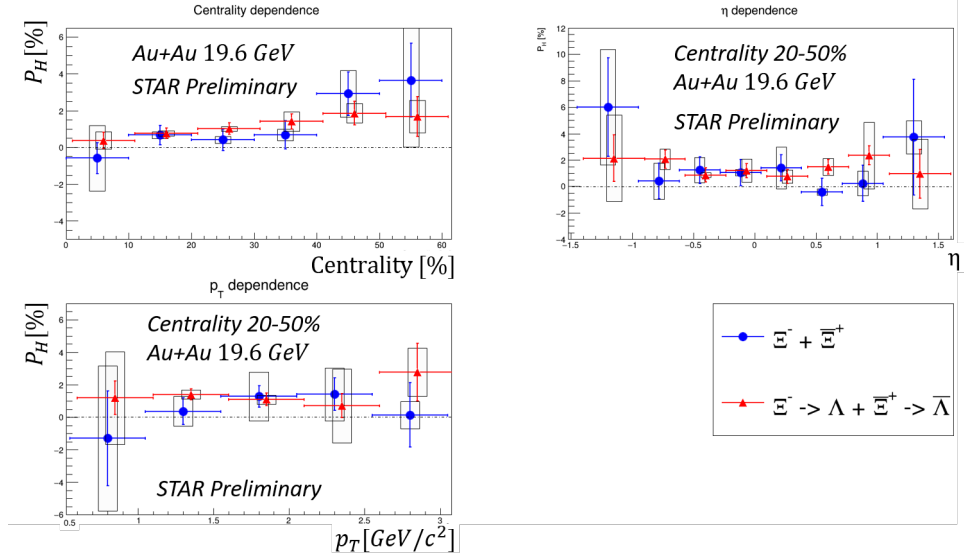


Fig. 2. Global polarization of Ξ hyperons in $\sqrt{s_{NN}} = 19.6$ GeV Au+Au collisions.

89 be rewritten as:

$$\frac{8}{\pi\alpha_H} \langle \sin(\phi_b^* - \Psi_{RP}) \rangle = \frac{4}{\pi} \overline{\sin\theta_b^*} P_H(p_t^H, \eta^H) = A_0(p_t^H, \eta^H) P_H(p_t^H, \eta^H), \quad (3)$$

90 where θ_b^* is polar angle of daughter baryon in parent's rest frame and $A_0(p_t^H, \eta^H) =$
 91 $\frac{4}{\pi} \overline{\sin\theta_b^*}$ is correction factor depending on p_t^H, η^H and collision centrality.

92

Results

93 Figure 2 and 3 presents global polarization of $\Xi^- + \Xi^+$ hyperons mea-
 94 sured directly and via daughter global polarization as a function of collision
 95 centrality, p_T and η for $\sqrt{s_{NN}} = 19.6$ and 27 GeV. Directly measured global
 96 polarization is consistent with measurements via daughter's global polariza-
 97 tion. Global polarization increases with centrality as expected from theoret-
 98 ical predictions and and previous Λ global polarization measurements. No
 99 obvious p_T or η dependence of global polarization observed.

100 Figure 4 shows polarization as a function of collision energy. The results
 101 of this analysis are shown together with that from $\sqrt{s_{NN}} = 7.7-200$ GeV Λ
 102 global polarization studies, BES-II Λ polarization results at $\sqrt{s_{NN}} = 19.6$
 103 and 27 GeV and the first $\sqrt{s_{NN}} = 200$ GeV study of Ξ global polarization.
 104 Theoretical curves obtained from AMPT [19] model are shown together with
 105 the experimental results. The global polarization of cascade follows a similar
 106 trend as observed for Λ and is consistent with theoretical AMPT calculations,
 107 which indicate global nature of hyperon global polarization.

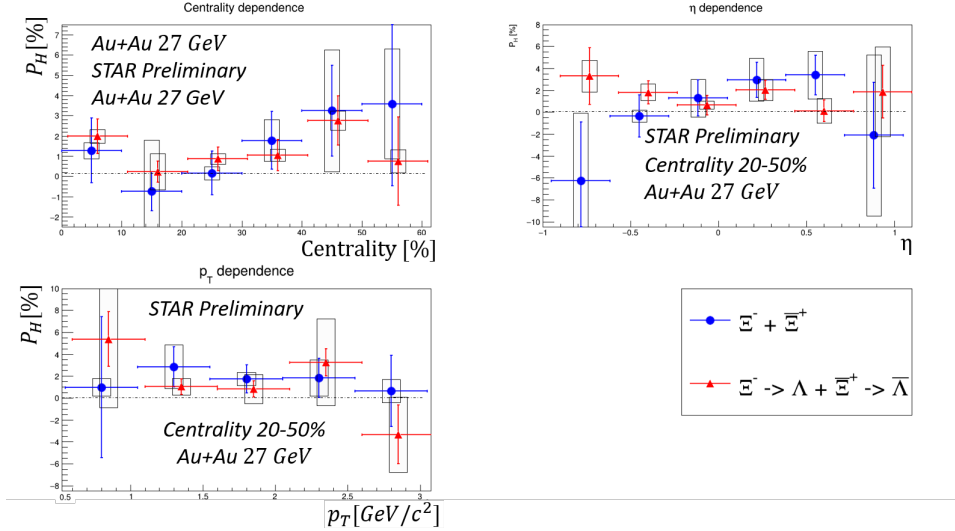


Fig. 3. Global polarization of Ξ hyperons in $\sqrt{s_{NN}} = 27$ GeV Au+Au collisions.

109 We presented the results of global polarization measurements for $\Xi^- + \Xi^+$
 110 in Au+Au collisions at $\sqrt{s_{NN}} = 19.6$ and 27 GeV measured directly via the
 111 angle of daughter Λ and via transfer to Λ daughter global polarization. Re-
 112 sults stay within experimental trend and consistent with theoretical predic-
 113 tions within uncertainties.

114 REFERENCES

- 115 1. *Voloshin S.A., Poskanzer A.M., Snellings R.* Collective phenomena in
 116 non-central nuclear collisions. 2008. arXiv:0809.2949 [nucl-ex].
- 117 2. *Liang Z.T., Wang X.N.* Globally Polarized Quark-Gluon Plasma in Non-
 118 central $A + A$ Collisions // Phys. Rev. Lett. 2005. Mar. V. 94. P. 102301.
 119 URL: <https://link.aps.org/doi/10.1103/PhysRevLett.94.102301>.
- 120 3. *Voloshin S.A.* Polarized secondary particles in unpolarized high energy
 121 hadron-hadron collisions? 2004. arXiv:nucl-th/0410089.
- 122 4. *Voloshin S.A., Niida T.* Ultrarelativistic nuclear collisions: Direction of
 123 spectator flow // Phys. Rev. C. 2016. Aug. V. 94. P. 021901. URL:
 124 <https://link.aps.org/doi/10.1103/PhysRevC.94.021901>.
- 125 5. *Zyla P.A. et al.* [Particle Data Group Collaboration] Review of Par-
 126 ticle Physics // Progress of Theoretical and Experimental Physics. 2020.
 127 08. V. 2020, no. 8. 083C01 [https://academic.oup.com/ptep/article-](https://academic.oup.com/ptep/article-pdf/2020/8/083C01/34673722/ptaa104.pdf)
 128 [pdf/2020/8/083C01/34673722/ptaa104.pdf](https://academic.oup.com/ptep/article-pdf/2020/8/083C01/34673722/ptaa104.pdf).
- 129 6. *Abelev B.I., Aggarwal M.M., Ahammed Z., Anderson B.D., Arkhip-*
 130 *kin D., Averichev G.S., Bai Y., Balewski J., Barannikova O.,*

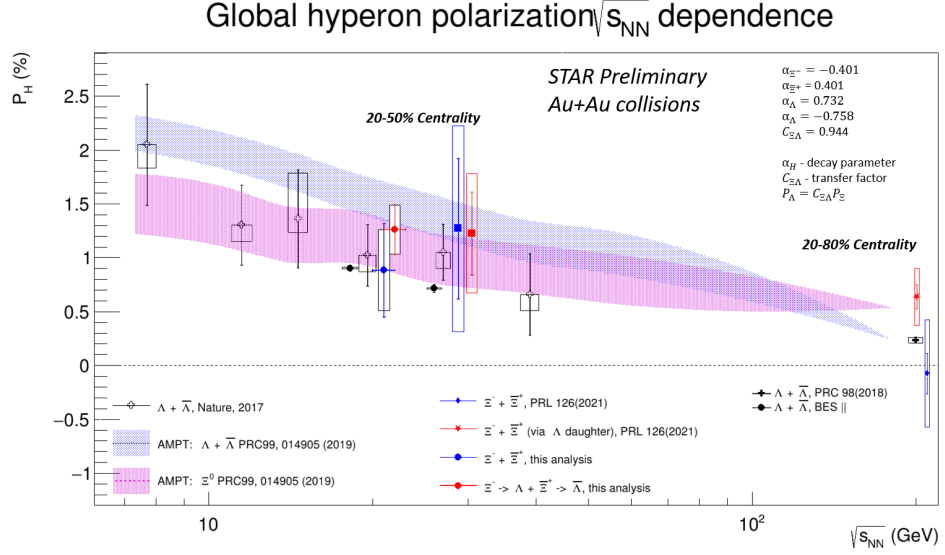


Fig. 4. Energy dependence of hyperon global polarization

- 131 *Barnby L.S., et al.* Global polarization measurement in Au+Au collisions // Physical Review C. 2007. Aug. V. 76, no. 2. URL:
 132 <http://dx.doi.org/10.1103/PhysRevC.76.024915>.
 133
- 134 7. *Adamczyk L., et al.* Global Lambda hyperon polarization in nuclear
 135 collisions // Nature. 2017. Aug. V. 548, no. 7665. P. 62–65. URL:
 136 <http://dx.doi.org/10.1038/nature23004>.
- 137 8. *Abdallah M.S. et al.* [STAR Collaboration] Global Λ -hyperon polarization
 138 in Au+Au collisions at $\sqrt{s_{NN}} = 3$ GeV. 2021. 7. arXiv:2108.00044.
- 139 9. *Adam J. et al.* [STAR Collaboration Collaboration] Global Polar-
 140 ization of Ξ and Ω Hyperons in Au + Au Collisions at $\sqrt{s_{NN}} =$
 141 200 GeV // Phys. Rev. Lett. 2021. Apr. V. 126. P. 162301. URL:
 142 <https://link.aps.org/doi/10.1103/PhysRevLett.126.162301>.
- 143 10. *Lee T.D., Yang C.N.* General Partial Wave Analysis of the Decay of a
 144 Hyperon of Spin $\frac{1}{2}$ // Phys. Rev. 1957. Dec. V. 108. P. 1645–1647. URL:
 145 <https://link.aps.org/doi/10.1103/PhysRev.108.1645>.
- 146 11. *Huang M. et al.* [HyperCP Collaboration] New Measurement of $\Xi^- \rightarrow$
 147 $\Lambda\pi^-$ Decay Parameters // Phys. Rev. Lett. 2004. Jun. V. 93. P. 011802.
 148 URL: <https://link.aps.org/doi/10.1103/PhysRevLett.93.011802>.
- 149 12. *Luk K.B., Diehl H.T., Duryea J., Guglielmo G., Heller K., Ho P.M.,*
 150 *James C., Johns K., Longo M.J., Rameika R., et al.* Search for Di-
 151 rectCPViolation in Nonleptonic Decays of Charged Ξ and Λ Hyperons //
 152 Physical Review Letters. 2000. Dec. V. 85, no. 23. P. 4860–4863. URL:
 153 <http://dx.doi.org/10.1103/PhysRevLett.85.4860>.

- 154 13. *Anerella M., et al.* The RHIC magnet system // Nuclear Instruments and
155 Methods in Physics Research Section A: Accelerators, Spectrometers, Detec-
156 tors and Associated Equipment. 2003. V. 499, no. 2. P. 280 – 315. The
157 Relativistic Heavy Ion Collider Project: RHIC and its Detectors URL:
158 <http://www.sciencedirect.com/science/article/pii/S016890020201940X>.
- 159 14. *Adams J., Ewigleben A., Garrett S., He W., Huang T., Jacobs P., Ju X.,*
160 *Lisa M., Lomnitz M., Pak R., et al.* The STAR event plane detector //
161 Nuclear Instruments and Methods in Physics Research Section A: Accelerators,
162 Spectrometers, Detectors and Associated Equipment. 2020. Jul. V. 968.
163 P. 163970. URL: <http://dx.doi.org/10.1016/j.nima.2020.163970>.
- 164 15. *Whitten C.A. et al.* [STAR Collaboration] The beam-beam counter: A
165 local polarimeter at STAR // AIP Conf. Proc. 2008. V. 980, no. 1.
166 P. 390–396.
- 167 16. *Anderson M., Berkovitz J., Betts W., Bossingham R., Bieser F., Brown*
168 *R., Burks M., Calderón de la Barca Sánchez M., Cebra D., Cherney M.,*
169 *et al.* The STAR time projection chamber: a unique tool for studying
170 high multiplicity events at RHIC // Nuclear Instruments and Methods
171 in Physics Research Section A: Accelerators, Spectrometers, Detectors and
172 Associated Equipment. 2003. Mar. V. 499, no. 2-3. P. 659–678. URL:
173 [http://dx.doi.org/10.1016/S0168-9002\(02\)01964-2](http://dx.doi.org/10.1016/S0168-9002(02)01964-2).
- 174 17. *Llope W.* Multigap RPCs in the STAR experiment at RHIC //
175 Nuclear Instruments and Methods in Physics Research Section
176 A: Accelerators, Spectrometers, Detectors and Associated Equip-
177 ment. 2012. V. 661. P. S110–S113. X. Workshop on Resist-
178 ive Plate Chambers and Related Detectors (RPC 2010) URL:
179 <https://www.sciencedirect.com/science/article/pii/S0168900210017006>.
- 180 18. *Maxim Z.* Online selection of short-lived particles on many-core computer
181 architectures in the CBM experiment at FAIR // Ph.D. thesis, Johann
182 Wolfgang Goethe-367 Universitat. 2016.
- 183 19. *Wei D.X., Deng W.T., Huang X.G.* Thermal vorticity and spin polariza-
184 tion in heavy-ion collisions // Phys. Rev. C. 2019. Jan. V. 99. P. 014905.
185 URL: <https://link.aps.org/doi/10.1103/PhysRevC.99.014905>.